

Preliminary design study on a Multi-Megawatts Fossil-based Supercritical CO₂ Recompression and Reheat Integral Test Facility

Hongzhi Li

Xi'an Thermal Power Research Institute Co., Ltd.

Xi'an, P. R. China

lihongzhi@tpri.com.cn

Wei Gao

Xi'an Thermal Power Research Institute Co., Ltd.

Xi'an, P. R. China

gaowei@tpri.com.cn

Yifan Zhang

Xi'an Thermal Power Research Institute Co., Ltd.

Xi'an, P. R. China

zhangyifan@tpri.com.cn

Mingyu Yao

Xi'an Thermal Power Research Institute Co., Ltd.

Xi'an, P. R. China

yaomingyu@tpri.com.cn



Hongzhi Li

Dr. Li is a *senior engineer working in Xi'an Thermal Power Research Institute Co., Ltd. Ph.D. of Power Engineering and Engineering Thermophysics, Xi'an Jiaotong University. Research on S-CO₂ power cycle and supercritical fluid heat transfer.*



Yifan Zhang

Engineer working in Xi'an Thermal Power Research Institute Co., Ltd. PH.D. of Power Engineering and Engineering Thermophysics, Xi'an Jiaotong University. Research on multi-phase flow and heat transfer, optimization design of heat exchanger.



Wei Gao

Engineer working in Xi'an Thermal Power Research Institute Co., Ltd. PH.D. of Jet Propulsion, Beihang University. Research on ORC and solar energy.



Mingyu Yao

Senior engineer working in Xi'an Thermal Power Research Institute Co., Ltd. Ph.D. of Power Engineering and Engineering Thermophysics, Xi'an Jiaotong University. Research on clean combustion of fossil fuels and pollution control methods.

Abstract:

The state of the art power conversion efficiency of the large scale ultra-supercritical fossil-fired steam power plant could achieve more than 44%. However, the technology bottleneck to further increase the efficiency seems difficult to breakthrough since expensive nickel-based alloys have to be used and thus overwhelmingly increase the cost of the plant. The alternative solution is to employ supercritical CO₂ (SCO₂) cycle due to its high efficiency and compact plant components. It exists great potential that the advanced SCO₂ plant efficiency could exceed 50% at 620°C without employment of the nickel-based alloys. The concept of the SCO₂ power cycle has been proved by several small scale test loops around the world. However, the multi-megawatts intermediate-scale test loop is still needed to demonstrate commercial viability of large scale technologies. Xi'an Thermal Power Research Institute (TPRI) is one of the top research organizations in the field of the fossil-fired power conversion technologies in China. TPRI are planning to develop SCO₂ power cycle technologies aimed to fossil-fired utility power plant. In the present paper the technology adaption, strengths, challenges and economic feasibility of SCO₂ power cycle for fossil-fired power plant have been evaluated. The preliminary design of a multi-megawatts fossil-based SCO₂ recompression and reheat integral test facility is presented. The turbine inlet temperature is expected to 600°C and the pressure is 20MPa. The operating parameters of the system and key components are evaluated and optimized by an in-house code. The effect of the key parameters such as split ratio, pressure ratio and reheat pressure are analyzed for the optimization design of the test facility. Furthermore, the preliminary design of the key components such as boiler, turbine, compressor and compact heat exchanger has been accomplished and the specifications of these components are presented in the present paper.

1. Introduction

The state of the art power conversion efficiency of the large scale ultra-supercritical fossil-fired steam power plant could achieve more than 44%. However, the technology bottleneck to further increase the efficiency seems difficult to breakthrough since expensive nickel-based alloys have to be used and thus overwhelmingly increase the cost of the plant. Carbon dioxide, due to its non-toxicity, non-flammability, abundance and low cost, is an economic competitive and environmental favorable working fluid. Supercritical Carbon dioxide Brayton Cycle (SCO₂-BC), in view of its simple system layout, superior cycle efficiency, compact plant components, and friendly environmental influence, have currently received significant attention and being studied for widely applications in nuclear, fossil, concentrating solar power (CSP), waste heat recovery and ship propulsion systems[1-10]. The SCO₂-BC is operated above the critical pressure of CO₂ (7.37MPa), where the fluid experiences no phase change, which leads to a simplified plant layout since there is no need for condensing systems. By virtue of small density change for different pressures near the critical point, the compressor work could be significantly reduced leading to higher cycle efficiency compared to the conventional supercritical steam Rankine cycle at the temperatures ranging from 450°C to 650°C[8-9], which is of the primary interests for

fossil, nuclear, and CSP. Furthermore, thanks to the high specific heat capacity near the pseudo-critical temperature (which is defined as the temperature, for a given pressure, at which the specific heat exhibits a maximum), the size of the system components could be minimized, indicating reduced the capital cost. In addition, the simplicity and compactness of $\text{SCO}_2\text{-BC}$ would also result in reduced installation, maintenance and operation costs of the plant.

The concept of the SCO_2 power cycle has been proved by several small scale test loops around the world. However, the multi-megawatts intermediate-scale test loop is still needed to demonstrate commercial viability of large scale technologies. Xi'an Thermal Power Research Institute (TPRI) is one of the top research organizations in the field of the fossil-fired power conversion technologies in China. TPRI are planning to develop SCO_2 power cycle technologies aimed to fossil-fired utility power plant. In the present paper the technology adaption, strengths, challenges and economic feasibility of SCO_2 power cycle for fossil-fired power plant have been evaluated. The preliminary design of a multi-megawatts fossil-based SCO_2 recompression and reheat integral test facility is presented. The turbine inlet temperature is expected to 600°C and the pressure is 20MPa. The operating parameters of the system and key components are evaluated and optimized by an in-house code. The effect of the key parameters such as split ratio, pressure ratio and reheat pressure are analyzed for the optimization design of the test facility. Furthermore, the preliminary design of the key components such as boiler, turbine, compressor and compact heat exchanger has been accomplished and the specifications of these components are presented in the present paper.

2. Cycle modeling and parameters thermodynamic analysis

An in house code was developed in FORTRAN in order to perform the cycle calculations and analyze the effect of the key parameters. The code consists of several subroutines to model the key components such as compressors, turbines and heat exchangers. Heat exchangers can be divided into recuperators, precoolers and intermediate heat exchangers. Recuperators (i.e. working fluid on both sides, but does not necessarily have the same mass flow rate) are used to preheat the working fluid before it enters into the intermediate heat exchangers. Precoolers (i.e. working fluid on one side and cooling medium, usually water, on the other) are used to reject heat from the cycle. Intermediate heat exchangers (i.e. fossil-fired boiler) are used for heat addition into the cycle. Both the simple and the recompression Brayton cycle layout could be easily modeled by combination of different components subroutines.

The recompression and reheat cycle has the biggest potential for efficiency improvement. The cycle layout is shown in Figure 1. This cycle layout improves efficiency by reducing the heat rejection from the cycle by introducing a recompressing compressor before the precoolers as well as by adding a reheater to increase working fluid temperature before it enters the low pressure turbine. A fraction of the working fluid is compressed to a high pressure within the main compressor (point 1 to point 2) and then it is preheated to the recompressor outlet temperature (point 2 to point 3'). Then the working fluid is merged with another fraction of the fluid flow from the recompressor (point 3'' to point 3). After that it flows into the high temperature recuperator and is preheated to the boiler inlet temperature (point 3 to point 4).

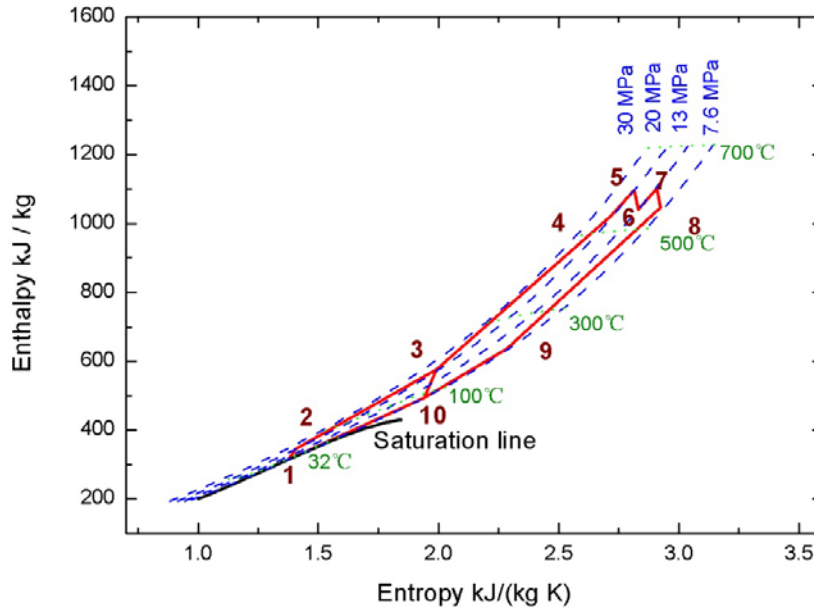


Figure 2 Enthalpy-Entropy diagram of the cycle

The effect of several major operating parameters that are used to improve cycle efficiency should be investigated. **When one parameter varied, the other parameters are kept constant.** **The baseline values of parameters are listed in Table 1.** Figures 3-4 show the cycle efficiencies for high pressure turbine and low pressure turbine inlet temperatures respectively under the conditions of two different split ratio to recompressor. The figures clearly indicate that increasing the turbine inlet temperatures improves the cycle efficiency almost linearly. This is not a surprising result since by increasing the turbine inlet temperature, the underlying thermodynamic efficiency of the cycle is improved.

Figure 5 shows the effect of High pressure turbine inlet pressure (or system pressure ratio) on the cycle efficiency. It could be seen that for a given working conditions with constant split ratio there exists an optimum turbine inlet pressure. If the split ratio could be adjusted with the increasing pressure ratio, the cycle efficiency could also be improved. But unlike the temperature, the beneficial effect of the turbine inlet pressure increase saturates and is less than a percent for a pressure increase from 25MPa to 30MPa.

Figure 6 shows the effect of low pressure turbine inlet pressure on the cycle efficiency. The low pressure turbine inlet pressure indicates the proportion of expansion work be allocated between the high pressure turbine and the low pressure turbine. For a given working condition there exists an optimum value. This value depends on the low pressure turbine inlet temperature, the two turbine efficiencies and the whole expansion ratio.

Figure 7 shows the effect of split ratio to recompressor on the cycle efficiency. It could be seen that for a given working condition there exists an optimum flow split ratio to the recompressor. The optimum value is decreased with the increase of the pressure ratio.

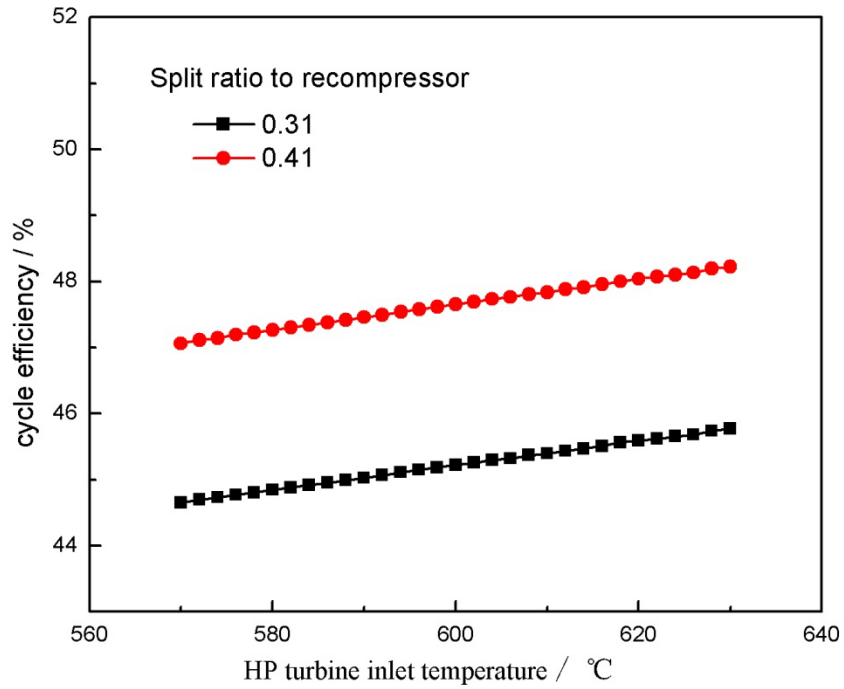


Figure 3 the effect of high pressure turbine inlet temperature on the cycle efficiency

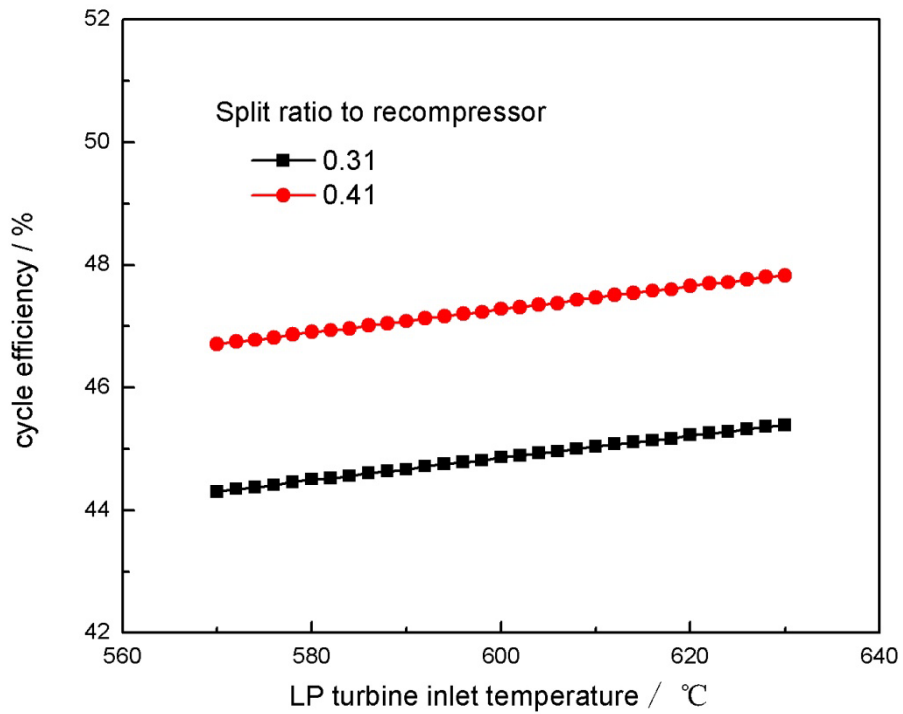


Figure 4 the effect of low pressure turbine inlet temperature on the cycle efficiency

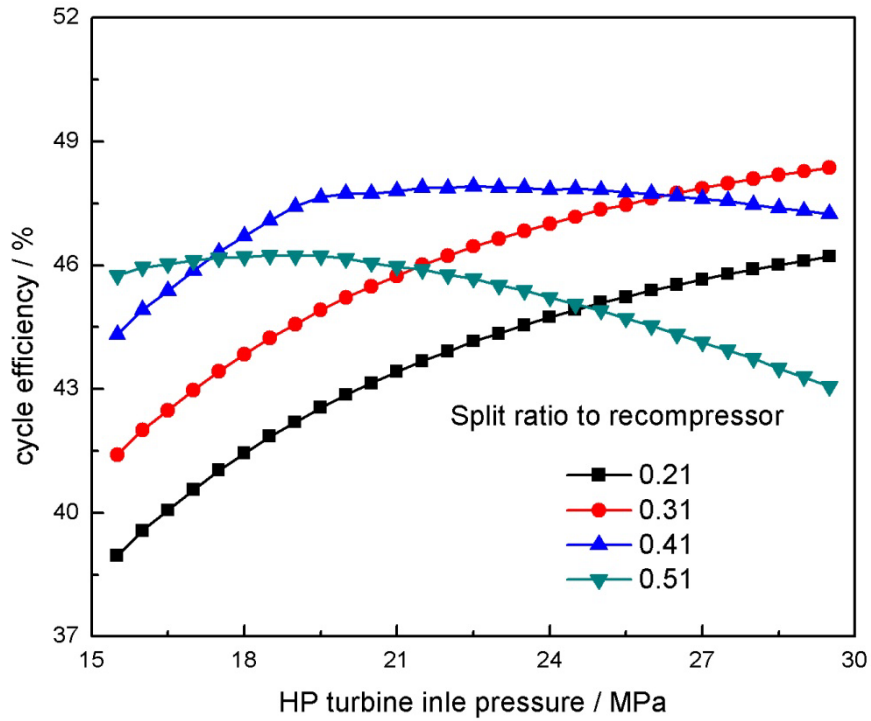


Figure 5 the effect of High pressure turbine inlet pressure on the cycle efficiency

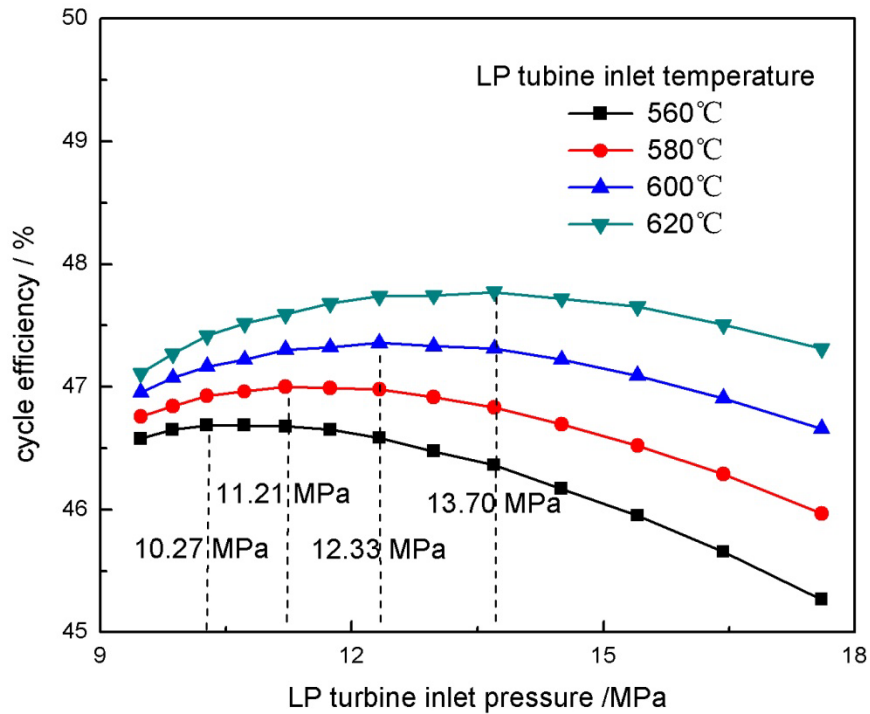


Figure 6 the effect of low pressure turbine inlet pressure on the cycle efficiency

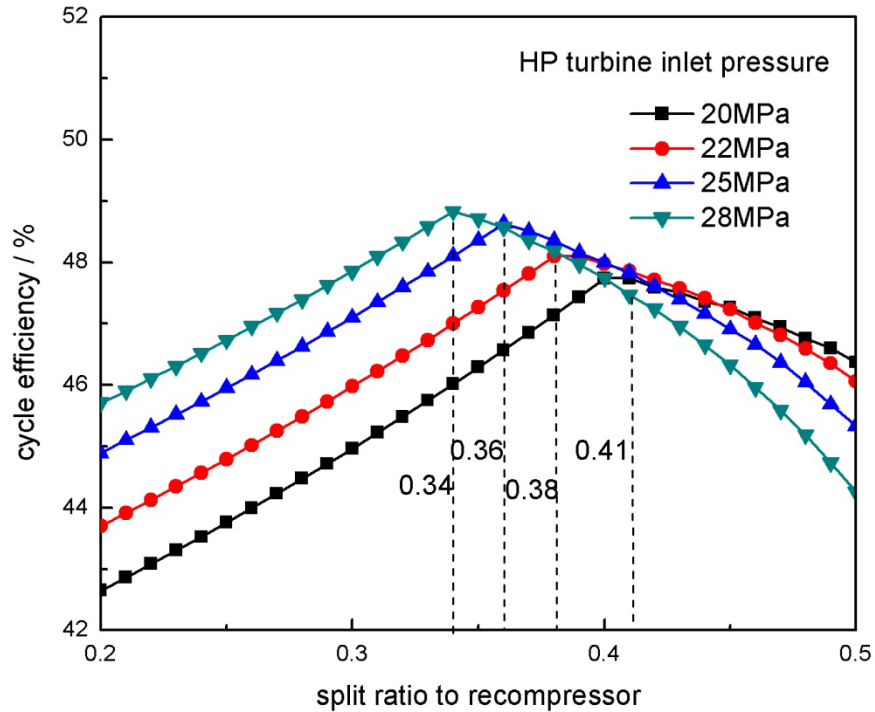


Figure 7 the effect of split ratio to recompressor on the cycle efficiency

3. Integral test facility layout

A Solidworks depiction of the recompression and reheat integral test loop design is presented in Figure 8. The dimensions of the whole test facility are 50m in length \times 20m in width \times 10m in height. The key hardware includes two turbine-alternator-compressors (high pressure turbine with main compressor; low pressure turbine with recompressor), two Printed Circuit Heat Exchanger (PCHE) recuperators, one PCHE precooler, one fossil fired boiler, CO₂ inventory expansion control system, circulation cooling water system, electrical power dissipation load banks and their controlling architectures located in the central control room. Note that certain auxiliary components such as the supporting skid, the boiler combustion system and electrical power dissipation load banks are omitted from this figure.

Table 1 gives a summary of the preliminary design value of certain parameters. The objective of the net capacity for this integral test facility is 5MWe. The main compressor inlet pressure and temperature was selected with 7.6MPa and 32 °C. The maximum turbine inlet pressure and temperature was designed by 20MPa and 600°C. The reheat pressure and temperature was 12.69MPa and 600°C. The efficiencies of the boiler, two turbines and compressors were assumed to 94%, 80-82% and 70-72% for such a small test loop. The optimum split ratio to the recompressor under this working condition is 0.384. In order to reduce the exhausted flue gas temperature in the boiler, a fraction of the flow was split from the inlet of the high pressure side of the high temperature recuperator to the economizer. The optimum flow split ratio to the economizer is approximate 0.08. The pressure drop within the boiler, reheating boiler, high temperature recuperator, low temperature recuperator and precooler is assumed with 0.8MPa,

0.4MPa, 0.3MPa and 0.1MPa respectively. Under this working condition the gross cycle efficiency is calculated with 32.29%.

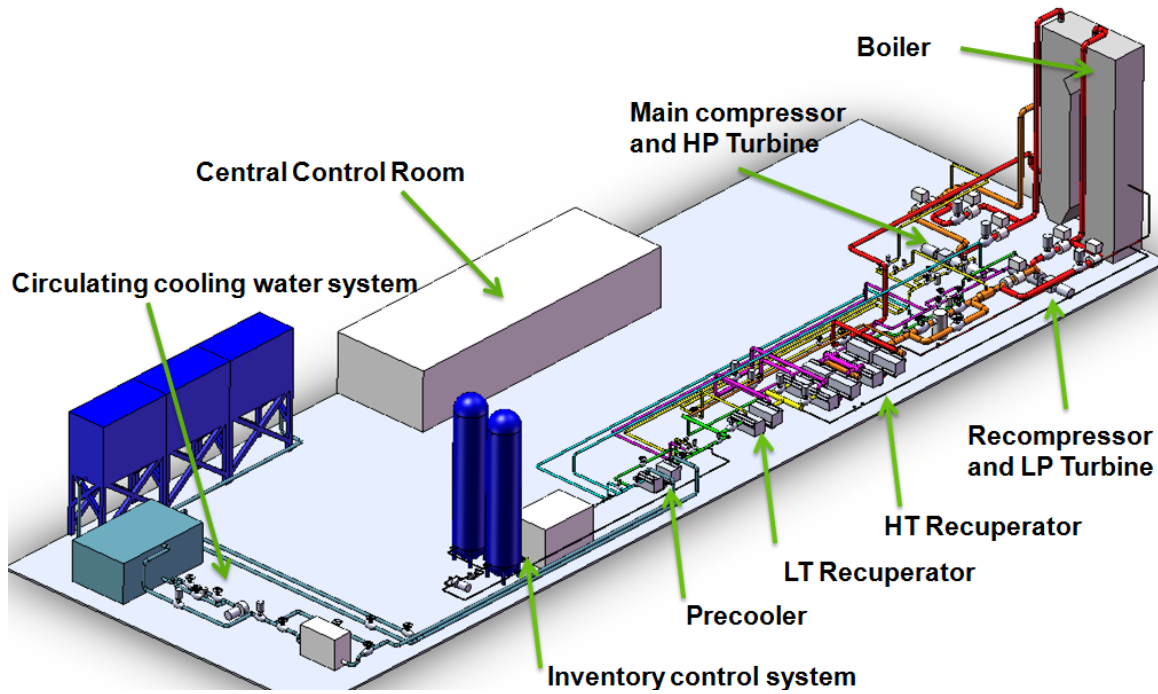


Figure 8 Schematic layout of the SCO₂-BC integral test facility

Table 1 summary of the preliminary design value of certain parameters

SR to Recompressor	/	0.384	HPT work	MW	4.687
SR to Economizer	/	0.08	LPT work	MW	4.75
HPT-IP	MPa	20	MC work	MW	1.588
HPT-IT	°C	600	RC work	MW	2.643
HP expansion ratio	/	1.527	Boiler duty	MW	14.557
LPT-IP	MPa	12.69	LTR duty	MW	12.011
LPT-IT	°C	600	HTR duty	MW	34.586
LP expansion ratio	/	1.527	PC duty	MW	9.351
MC-IP	MPa	7.6	Net capacity	MWe	5
MC-IT	°C	32	Boiler efficiency	%	94
MC PR	/	2.816	MC efficiency	%	70

RC-IP	MPa	7.71	RC efficiency	%	72
RC-IT	°C	80.085	LPT efficiency	%	82
RC PR	/	2.737	HPT efficiency	%	80
Mass Flow Rate	t/h	304.37	Cycle gross efficiency	%	32.29

4. Fossil-fired boiler

Figure 9 and Table 2 show preliminary design results of the fossil-fired boiler specifically for the integral test facility. The fuel is oil with the following composition: C: 83.976%; H: 12.23%; O: 0.568%; N: 0.2%; S: 1%; ash: 0.026%; water: 2%, LHV: 41860kJ/kg. The temperature in a fossil fired boiler is around 1400 °C and approximately half the total heat duty is delivered at this temperature through radiative heat transfer, the other half is the sensible heat of flue gas through convective heat transfer. The CO₂ cycle heating must be designed specifically for a fossil fired boiler. The heat needed for the cycle is delivered at high temperature (i.e. above 500°C) consequently a large part of the heat duty in the flue gas below 500°C cannot be fully utilized in the CO₂ cycle or by air preheating. In order to address this problem an additional split flow CO₂ economizer has been added before the air preheater. Moreover, in order to maximize efficiency and use the high heat transfer in the boiler, one reheat have been added. The maximal cycle temperature is 600°C which is almost equal to the maximum temperature in most advanced supercritical steam/water power cycle (30MPa/600°C/620°C).

The boiler has been designed as a tangentially fired π boiler. The combustion residence time combined with the disengagement zone residence time has been set to 1.3s with a maximal flue gas velocity of 7 m/s at the furnace outlet. A 10% overdesign has been added. The proposed design shows a 9.5m in height and the cross section is a 2x2m square. Due to the high average temperature of cooling media in the furnace (around 550°C) a high metal temperature (around 620°C) is reached therefore a very high grade of martensitic steel (e.g. T91) must be used for flue gas corrosion protection. The superheater and reheater are made of super 304H austenitic steel. This grade of steel allows an operating pressure of 20MPa at relatively little cost. Due to the high amount of radiative heat released in the furnace and the high average temperature of the supercritical CO₂, the furnace wall are used for both the primary heat and reheat cooling walls.

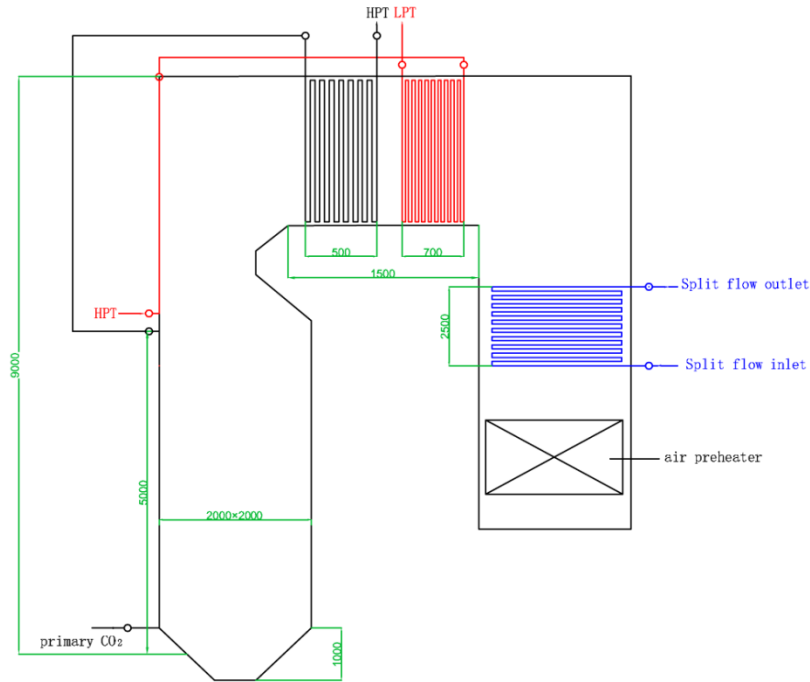


Figure 9 Schematic layout of the preliminary design of the fossil fired boiler

Table 2 summary of the preliminary design of the fossil fired boiler

		FWSH	FWRH	SH	RH	ECO	APH
Heat Duty	kW	4809	3983	1590	989	3005	1746
Heating surface Area	m ²	39.6	32.8	63	89	315	1403
flue gas IT	°C			1012.7	854.6	733.8	351.1
flue gas OT	°C			854.6	733.8	351.1	118.7
CO ₂ /air IT	°C	538.8	551.3	584.3	589.7	193.5	25
CO ₂ /air OT	°C	584.3	589.7	600	600	538.7	290.8
flue gas velocity	m/s			14.89	13.27	12.57	10.7
CO ₂ velocity	m/s			23.67	19.78	4.95	5.83
LMTD	°C			334.4	194.6	175.7	63.2
tube outside diameter	mm	25	25	42	42	38	38
tube thickness	mm	5	4	5	4	4	2
Outside wall temperature	°C	621	611	605	590	550	
volume	m ³	0.212	0.225	0.384	0.612	1.865	/
weight	t	2.939	2.045	2.165	2.512	8.793	21.89

5. Turbomachinery

The recompression cycle has two rotational shafts (compressor-turbine-gearbox-generator),

which have similar layout. One compressor connected to one turbine which is coupled with a motor/generator through a gearbox reducing high rotational speed (30000RPM) to the conventional industry 3000RPM. The shaft is driven by a motor/generator control box capable of power levels matching the range of operation. It is designed to allow seamless transition during operation from motoring to generating.

There are two compressors in the test loop. The main compressor was designed to operate near the critical point where fluid density is high and viscosity comparatively low in order to minimize the required compression work, resulting in a benefit to the overall efficiency of the cycle. Due to its proximity to the critical point and potential for two-phase operation, the design of the main compressor is more complicated than the hot recompressor. Thus, in present paper we mainly focus on the preliminary design of the main compressor. The main compressor was designed for an inlet pressure and temperature of 7.6MPa and 32°C respectively, producing a discharge pressure of 21.4MPa at rotational speed of 30,000RPM. The main compressor mass flow rate of 52.08 kg/s in conjunction with a predicted design point efficiency of 70% yields a design power of 1.58 MW for this component. The design of rotational speed was limited to 30,000 RPM due to reliability and rotordynamic considerations. This results in a nondimensional specific speed of 0.53, which is less than the optimal value of approximately 0.74 for the given pressure ratio. One would expect higher efficiency if the speed could be increased, however, the benefit would be negated somewhat by the smaller wheel size and thus larger relative clearances that would result from a faster design speed.

A preliminary steady state CFD and FEM simulation for main compressor was performed and the results were shown in Figure 10. The density of supercritical CO₂ at the inlet of the main compressor is very dense, but the increase of the density and temperature are not so much in the working process. The calculated discharge pressure is 21.5MPa and the isentropic efficiency is 73%, which agree well with the assumption of the preliminary design. Considering corrosion resistance, high strength and lightness, the titanium alloy was selected as material for the supercritical CO₂ compressor impeller. Both the aerodynamic pressure and the centrifugal load should be considered together in the study of the stress of the supercritical CO₂ impeller. The von Mises stress of the supercritical CO₂ compressor impeller was presented in Figure. 10. The maximum von Mises stress under both pressure and centrifugal load is 622MPa, which is smaller than the allowable stress. The peak stress is located close to the leading edge at the blade root of the splitter blades.

A preliminary steady state CFD and FEM simulation for high pressure turbine was performed and the results were shown in Figure 11. The calculated turbine work is 4.6MW and the isentropic efficiency is 80%, which is almost the same with the design value. Inconel 718 was used for the turbine wheel material because of its ability to withstand high temperatures and stresses. Similarly, The von Mises stress of the supercritical CO₂ turbine impeller was presented in Figure. 11. The maximum von Mises stress under both pressure and centrifugal load is 433MPa, which is much smaller than the allowable stress. The peak stress is located close to the leading edge at the blade root of the blades.

A labyrinth seal together with a dry gas seal were used to make sure the leakage flow less than

0.1%. The tilting pad journal and thrust bearings were designed to withstand the axial and radial load. A preliminary rotordynamic analysis was also performed . The 1st and 2nd order critical speed were approximate 12000RPM and 38000RPM, respectively, indicating that the required shaft speed could safely operate within a wide range.

Table 3 summary of the preliminary design of compressors and turbines

	Unit	MC	RC	HPT	LPT
mass flow rate	kg/s	52.08	32.47	84.55	84.55
work	MW	1.58	2.64	4.68	4.75
impeller diameter	mm	140	200	120	200
inlet pressure	MPa	7.6	7.7	20	12.7
inlet temperature	°C	32	80	600	600
inlet density	kg/m ³	557.5	152.4	116.7	75.26
outlet pressure	MPa	21.4	21.1	13.09	8.31
outlet temperature	°C	70.1	187.3	551.3	551.1
outlet density	kg/m ³	684.6	288.58	82.4	52.76
shaft speed	rpm	30000	30000	30000	30000
isentropic efficiency	%	70	72	80	82

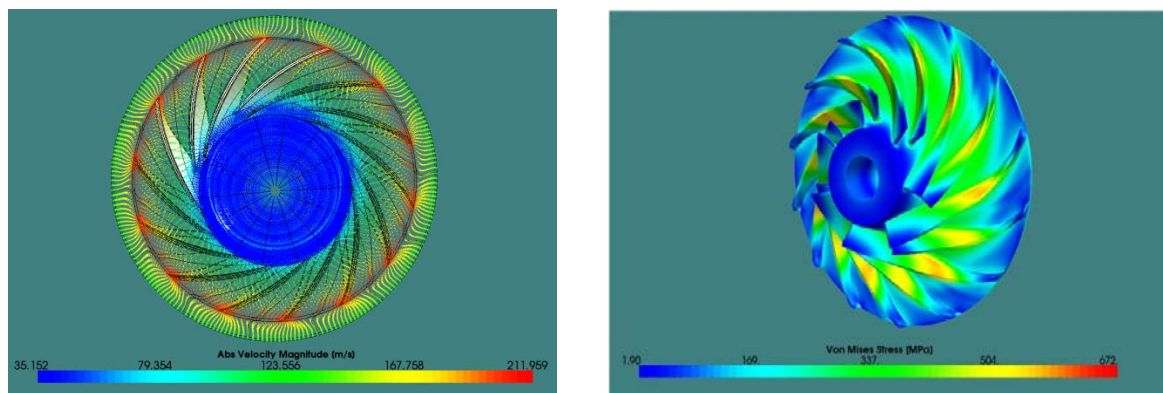


Figure 10 preliminary CFD and FEM simulation results of main compressor

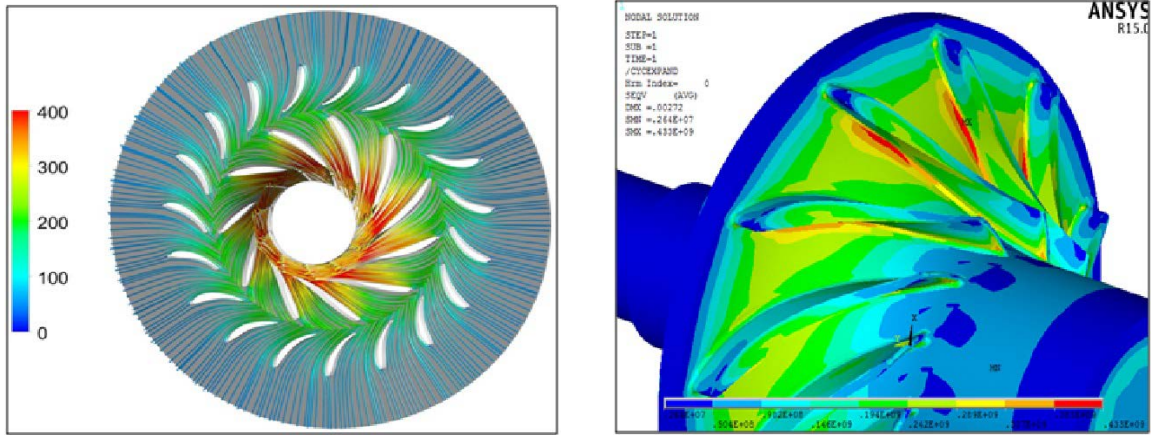


Figure 11 preliminary CFD and FEM simulation results of high pressure turbine

6. Printed circuit heat exchangers

The primary difference in the Supercritical CO₂ cycle that enables higher efficiency is the availability of a useful temperature difference between the exhausted working fluid exiting the turbine and the fresh working fluid exiting the compressor, which drives heat transfer through recuperation in the heat exchangers. Only a small amount of heat needs to be rejected from the cycle to get the Supercritical CO₂ at the right density to recompress it. Therefore, to achieve an efficient Supercritical CO₂ cycle, one of the major technical challenges exists in the highly effective recuperators design. To minimize capital costs, the printed circuit heat exchangers (PCHE), produced by large UA values, is created by photo-etching small flow channels into sheets of alloys. The metal layers are then diffusion bonded together. The PCHE gained significant popularity thanks to their compact nature[11-19]. This results in heat exchangers that are up to 85% smaller than the conventional shell and tube ones [18].

The performance of the PCHE plays a significant role in the cycle efficiency. The heat transfer behavior in the recuperators is significantly different from that of a constant property fluid. The radical change in physical properties near the critical point may limit the heat exchange rate of the PCHE due to the presence of a pinch point inside the regenerative heat exchanger. Therefore, it is of great interest and necessity to study such heat transfer regime and to evaluate the local heat transfer coefficient throughout the recuperators, which is of great importance in PCHE design and cycle optimization.

The approximate heat transfer and flow dimensions of the high temperature recuperator, low temperature recuperator and precooler are provided in Table 4. They are all constructed of 316 stainless steel. The high temperature recuperator was designed to transfer 34.58 MW at a flow rate of 84.55 kg/s with a hot-side inlet temperature of 551.1°C and a maximum allowable working pressure of 21.5 MPa. Whereas, the low temperature recuperator has a smaller size, approximate one fourth of the high temperature recuperator. The low temperature recuperator, as well as, the precooler need to be carefully designed for avoiding the pinch point inefficiency problem. Excess cycle heat energy is rejected at the precooler. The heat removal capacity of the precooler is approximately 9.5 MW, which is sufficient to establish the main

compressor inlet CO2 temperature near the critical temperature.

Table 4 summary of the preliminary design of recuperators and precooler

		HT Recup		LT Recup		PC	
		Hot	Cold	Hot	Cold	Hot	Cold
heat duty	MW	34.58		12.01		9.5	
heat transfer area	m ²	2460		837.4		360.59	
unit size	m	0.6×0.6×1.35		0.6×0.6×1.35		0.6×0.6×1.35	
number of unit	/	8		2		1	
U	W/(m ² K)	978.6		1215.4		2463.6	
average DT	K	15.84		12.31		25.83	
Volume	m ³	1.4		0.52		0.14	
Weight	t	38		10.6		2.25	
WF		CO2	CO2	CO2	CO2	CO2	H2O
MFR	kg/s	84.55	77.78	84.55	52.08	52.08	110
PI	MPa	8.31	21.1	8.01	21.4	7.71	0.2
PO	MPa	8.01	20.8	7.71	21.1	7.6	0.11
TI	°C	551.1	187.3	197.4	70.1	80.1	20
TO	°C	197.4	540.1	80.1	187.3	32	32.5

7. Conclusions

TPRI are planning to develop SCO₂ power cycle technologies aimed to fossil-fired utility power plant. The preliminary design of a multi-megawatts fossil-based SCO₂ recompression and reheat integral test facility is presented. The turbine inlet temperature is expected to 600°C and the pressure is 20MPa. The operating parameters of the system and key components are evaluated and optimized by an in-house code. The effect of the key parameters such as split ratio, pressure ratio and reheat pressure are analyzed for the optimization design of the test facility. Furthermore, the preliminary design of the key components such as boiler, turbine, compressor and compact heat exchanger has been accomplished. The whole test facility was planned to built at the end of 2017.

Acknowledgements:

The authors acknowledge the financial support provided by the National Natural Science Foundation of China (Grant No. 51406166), Key Programs of China Huaneng Group (Grant No. HNKJ15-H07) and Yong Talent Programs of Chinese Society for Electrical Engineering.

References

- [1] B.D. Iverson, T.M. Conboy, J.J. Pasch, A.M. Kruizenga. Supercritical CO₂ Brayton cycles for solar-thermal energy. *Appl Energy* 2013; 111:957-70.
- [2] Y.L. Moullec. Conceptual study of a high efficiency coal-fired power plant with CO₂ capture using a supercritical CO₂ Brayton cycle. *Energy* 2013; 49:32-46.
- [3] R. Singh, S.A. Miller, A.S. Rowlands, P. A. Jacobs. Dynamic characteristics of a direct-heated supercritical carbon-dioxide Brayton cycle in a solar thermal power plant. *Energy* 2013; 50:194-204.
- [4] Y.M. Kim, C.G. Kim, D. Favrat. Transcritical or supercritical CO₂ cycles using both low- and high-temperature heat sources. *Energy* 2012; 43:402-15.
- [5] Dostal V. A supercritical carbon dioxide cycle for next-generation nuclear reactors. Ph.D. thesis, Department of Nuclear Engineering, MIT, USA; 2004.
- [6] Dostal V, Hejzlar P, Driscoll MJ. The supercritical carbon dioxide power cycle: comparison to other advanced power cycles. *Nuclear Technology* 2006; 154:283-301.
- [7] Feher EG. The supercritical thermodynamic power cycle. *Energy Conversion* 1968; 8:85-90.
- [8] Wright SA, Conboy TM, Carlson MD, Rochau G. High temperature split-flow re-compression Brayton cycle initial test results. SAND2012-5308349, July 2011, Sandia National Laboratories, Albuquerque, NM; 2011.
- [9] Pasch J, Conboy TM, Fleming DD, Rochau G. Supercritical CO₂ recompression Brayton cycle: completed assembly description. SAND2012-9546, October 2012, Sandia National Laboratories, Albuquerque, NM; 2012.
- [10] J. Sarkar. Second law analysis of supercritical CO₂ recompression Brayton cycle. *Energy* 2009; 34:1172-78.
- [11] Li H, Kruizenga A, Anderson M, Corradini M, Luo Y, Wang H, et al. Development of a new forced convection heat transfer correlation for CO₂ in both heating and cooling modes at supercritical pressures. *Int J Therm Sci* 2011; 50:2430-42.
- [12] Tsuzuki N, Kato Y, Ishizuka T. High performance printed circuit heat exchanger. *Appl Therm Eng* 2007; 27:1702-7.
- [13] Ngo TL, Kato Y, Nikitin K, Tsuzuki N. New printed circuit heat exchanger with S-shaped fins for hot water supplier. *Exp Therm Fluid Sci* 2006; 30:811-9.
- [14] Ngo TL, Kato Y, Nikitin K, Ishizuka T. Heat transfer and pressure drop correlations of microchannel heat exchangers with S-shaped and zigzag fins for carbon dioxide cycles. *Exp Therm Fluid Sci* 2007; 32:560-70.
- [15] Ishizuka T, Kato Y, Muto Y, Nikitin K, Tri Lam N. Thermal-hydraulic characteristics of a printed circuit heat exchanger in a supercritical CO₂ loop. *Bull Res Lab Nucl React* 2006; 30:109-16.
- [16] Kim DE, Kim MH, Cha JE, Kim SO. Numerical investigation on thermal-hydraulic performance of new printed circuit heat exchanger model. *Nucl Eng Des* 2008;238:3269–76.
- [17] Kim IH, No HC, Lee JI, Jeon BG. Thermal hydraulic performance analysis of the printed circuit heat exchanger using a helium test facility and CFD simulations. *Nucl Eng Des* 2009; 239:2399-408.

[18] Carlson MD, Kruienga AM, Anderson MH, Corradini ML. Heat transfer and pressure drop of supercritical carbon dioxide flowing in several printed circuit heat exchanger channel patterns. In: International congress on advances in nuclear power plants, June 24-28, 2012, Chicago, IL; 2012.

[19] J.D. Jackson. Fluid flow and convective heat transfer to fluids at supercritical pressure. Nucl Eng Des 2013; 264:24-40.